ARMA e-NEWSLETTER 22

AMERICAN ROCK MECHANICS ASSOCIATION • FALL 2017 • ISSUE 22

## In this issue





## Editor's Note

*This issue of the e-Newsletter is dedicated to highlights of the 2017 ARMA Rock Mechanics/Geomechanics Symposium held 25-28 June 2017 in San Francisco, California. We invited all keynote presenters to submit summaries of their lectures; three of them accepted our invitation, and their submissions are included herein. In addition, we offer highlights of the three workshops held during the weekend preceding the symposium, as submitted by the respective workshop organizers.*

*The main keynote, which goes by the name of The MTS Lecture, was given by Professor Francois Cornet, who discussed the limits of elasticity for modeling stress fields in geological formations, and the effect of gravity on an orthotropic visco-poro-elastic formation. He then proposed a new model for analyzing the regional stress field in intraplate regions where no tectonic activity is presently identified.*

*Dr. Maria Nikolinakou discussed the development of transient evolutionary models that couple three geologic processes: salt deformation, basin sedimentation, and porous fluid flow. These models enable the study of the kinematic evolution of a salt basin.*

*Professor Erik Westman described the history of seismic tomography, the concept behind using p-wave arrival times for mapping stress redistribution, and presented two examples of its usage in deep mines.*

*The Hydraulic Fracturing Workshop, organized by Dr. Gang Han, covered the wide range of uses that this unique technique facilitates, from the measurement of in situ stress at great depth, to production stimulation in sandstone formations, to making production possible in large shale deposits. The morning session advanced the understandings of the physics involved in hydraulic fracturing. The afternoon modeling session demonstrated the model capacity to capture recognized physics.*

*The Workshop on Emerging Advances in Geomechanics, organized by the ARMA Future Leaders community and reported by Dr. Ghazal Izadi, focused on multi-disciplinary problems of geomechanical engineering applications, including unconventional oil and gas production, mass mining processes, deep geothermal energy utilization, and underground storage of nuclear waste.*

*The Workshop on How Laboratory Geomechanics Testing Adds Value to Exploration and Production was organized by Dr. Abhijit Mitra. Several standard and specialized geomechanics testing techniques were presented, followed by quality control methods for reviewing test results. This was followed by ways to design a laboratory geomechanics program for a specific reservoir or operating environment. Examples of laboratory geomechanics studies benefitting exploration and production activity were provided.*

*For more complete reports on both the keynotes and the workshops, I invite you to read the summaries that follow.*

—Bezalel Haimson

# Vertical Stress Profiles and the Long-Term Rheology of Rock Masses

*Submitted by F.H. Cornet, EOST-Univ. de Strasbourg, France*

## 1. Introduction

Stress at a point is defined by a symmetrical tensor with six independent components, so that at any given time the regional stress field is described by six functions of time and three spatial coordinates.

In this article, we review various approaches that help produce these six functions, when time variations are neglected. This process is illustrated by two examples: one taken in a granite massif and one taken from the French Paris Basin sedimentary formations.

We also discuss the limits of elasticity for modeling stress fields in geological formations and the effect of gravity on an orthotropic visco-poro-elastic formation. The time dependency is linked to pressure solution and climatic variations.

This analysis helps us propose a new paradigm for analyzing the regional stress field in intraplate regions where no tectonic activity is presently identified.

## 2. Regional stress field evaluations

In a geographical frame of reference, it is very often convenient to characterize the stress tensor by the three angles that define the local principal stress directions and by the three principal stress components.

When topography effects may be neglected, one principal component of the regional stress field may be assumed a priori to be vertical (noted $\sigma_v$). The two other components are horizontal and noted respectively $\sigma_H$ and $\sigma_h$ for the maximum and the minimum horizontal components.

The world stress map (Zoback, 1992; Heidbach et al., 2010) proposes a compilation of all stress field evaluations that have been conducted in the world. This catalog should always be consulted before undertaking a local evaluation. It may help obtain useful information on the regional principal stress directions. (The 2016 release is available at *www.world-stress-map.org/)*.

Results are plotted on the assumption that one principal component is vertical. However, stress varies with depth, and for most engineering projects some precise estimation of these variations is necessary. This information may be derived from borehole investigations as well as from natural or induced micro-seismic analysis.

### 2.1 Geophysical borehole investigations for principal stress directions identification

Geophysical investigations include borehole wall imaging (ultrasonic or electrical techniques) as well as P and S wave velocity azimuthal variations as determined from specialized sonic logs.

Because boreholes perturb the regional stress field locally, identification of these perturbations may be used to advantage for identifying principal stress directions. When the borehole is parallel to a principal stress direction, the tangential component is maximum in the direction parallel to that of the minimum principal stress perpendicular to the borehole axis. It is minimum in the direction parallel to that of the maximum principal stress component normal to the borehole axis (e.g. Cornet [ch. 5], 2015; Zoback [ch. 6], 2010).

For azimuths where compression failure conditions are satisfied, breakouts may develop, and their mapping helps identify the orientation of the minimum principal stress orientation.

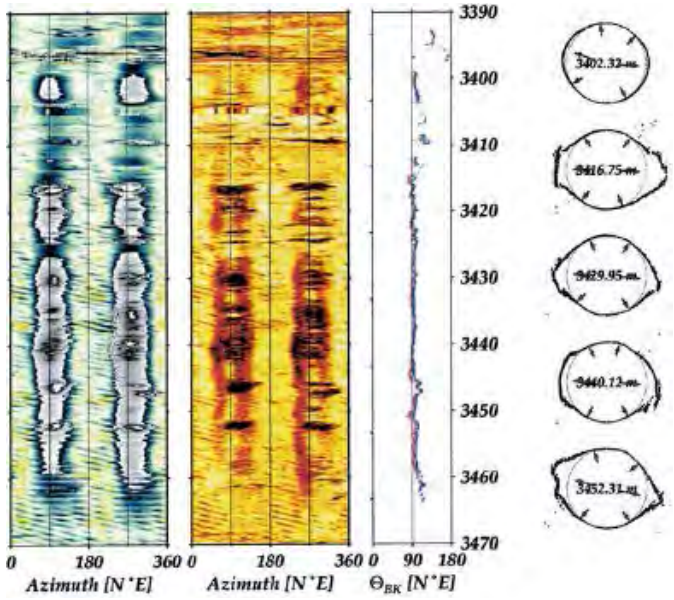


*Figure 1. Example of borehole breakouts in granite as mapped by ultrasonic imaging (Berard and Cornet, 2003).*

Similarly, at the points where the minimum tangential stress components satisfy tensile failure conditions, tensile fractures develop and their mapping yields the orientation of the maximum principal stress in the direction normal to the borehole axis.

When no failure develops, principal stress directions may be identified by investigating azimuthal variations in seismic velocity as identified with dipole sonic logs (Lei et al., 2012). Dipole sonic logs generate both P and S waves that propagate along the borehole axis. Because rocks always contain some micro-cracks, they exhibit a non-linear elastic response. Detection of directions for which seismic velocities reach extreme values help identify the far-field principal stress directions.

Because these logs cover long borehole lengths, they provide a unique evaluation of the stress field continuity. They also help identify main zones of heterogeneity. This information is essential for properly selecting zones for local hydraulic testing.

**2.2 Borehole hydraulic testing for a complete principal stress component evaluation**

- **The classical hydraulic fracturing technique**

A fracture-free portion in a borehole, parallel to a principal stress direction, is isolated with an inflatable straddle packer (example of packer pressure given by the top blue curve in Figure 2).

The isolated interval is then pressurized with a constant flow rate (lower part of Figure 2) until the borehole wall fractures. After the hydraulic fracture has been extended for a short distance, pressurization stops, and the drop in pressure is recorded (green curve, step 1, in Figure 2).

Then, after dropping the interval pressure to an arbitrary low value, injection is restarted at constant flow rate and the fracture is extended to a distance equal to four or five borehole diameters. Injection stops and the drop in pressure is recorded (green curve, step 2, in Figure 2).

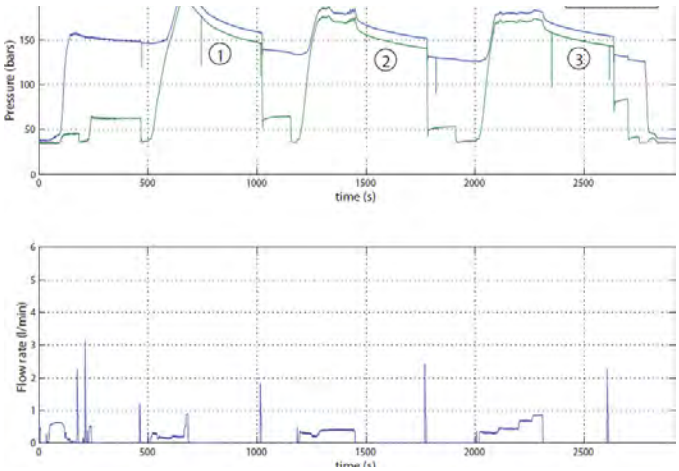


*Figure 2. Pressure and flow rate records for a classical hydraulic fracturing test (Cornet [chapt. 13], 2015)*

During step 3, the fracture is reopened with an injection flow rate increased step by step. When the flow rate increase does not significantly alter the interval pressure, injections stop and the drop in interval pressure is recorded.

Detailed analysis of the pressure drop observed during step 2 yields an upper bound and a lower bound to the so-called shut-in pressure (Haimson and Cornet, 2003). Analysis of the flow rate – pressure record observed during step 3 yields the quasi-static reopening pressure. The mean value between step 2 shut-in pressure and step 3 quasi-static reopening pressure may be considered a sound estimate of the far field minimum principal stress magnitude (Cornet et al., 2003).

The surge in pressure observed at the end of each step, after the interval pressure has been dropped suddenly, is caused by some fluid flow back to the packed off interval (Figure 2). It constitutes a useful test of the testing system tightness and provides a demonstration that the fracture has not extended axially beyond the packers.

The peak of interval pressure observed in step 1 (Figure 2) is called the breakdown pressure and is often used for determining the magnitude of the maximum principal stress component normal to the borehole axis. But, personally, I discourage this practice for the following four reasons.

First, in many cases, electrical images obtained just after testing have demonstrated that the fracture extends some distance along the packers and that most likely it has been initiated by the packers;

Second, when the stiffness of the testing system is not high enough, the fracture initiates sometime before the interval pressure reaches its peak. In fact, fracture occurs when the pressure-time curve becomes non-linear (Ito et al., 1999).

Third, permeability depends strongly on stress and therefore its characteristics vary with azimuth at the borehole wall. This creates difficulty for properly taking into account effects of pore pressure.

Finally, the mechanics of fracture initiation involve the growth of micro-cracks, the characteristics of which are generally unknown.

This introduces too many unknowns that hamper the reliability of such evaluations and alternative methods have been developed.

- **Hydraulic testing of preexisting fractures**

Laboratory experiments on hydraulic fracturing have

shown that, when pre-existing fractures exist in the packed-off interval, these fractures may, or may not, influence the formation of a new fracture, depending on flow rate (Cornet and Valette, 1984). This observation is taken to advantage with the hydraulic testing of pre-existing fractures (HTPF) method (Cornet, 1993).

The section of a borehole, where only one pre-existing fracture has been identified, is packed off with an inflatable straddle packer. The interval pressure is raised progressively, step by step, until the interval pressure-flow rate record changes slope significantly. When injection flow rate stops, the subsequent interval pressure drop is monitored. Analysis of the pressure drop yields an estimate of the shut-in pressure, which is taken equal to the normal stress, $\sigma_n(\underline{N})$, supported by the fracture with normal $\underline{N}$ away from the well:

$$\sigma_n(\underline{N}) = \sigma_{ij}\, N_i\, N_j, \qquad (1)$$

$\sigma_{ij}$, Ni, Nj are respectively the components of the far-field stress tensor (assumed to be uniform) and of the unit normal to the tested fracture, as expressed in the ($\mathbf{I_1}$, $\mathbf{I_2}$, $\mathbf{I_3}$) frame of reference.

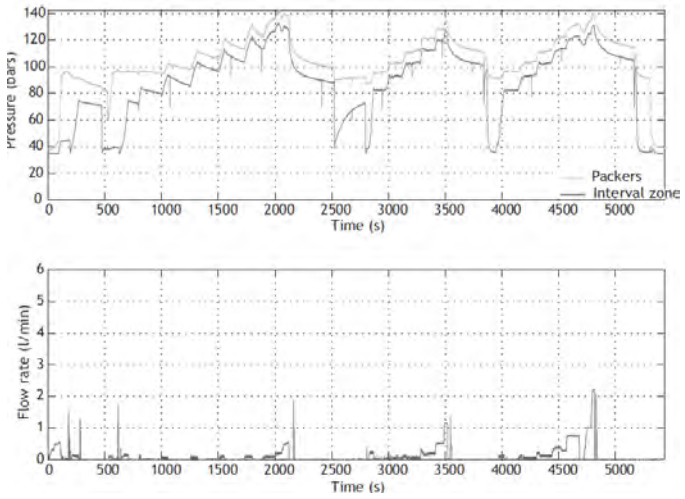


*Figure 3. Pressure and flow rate records for an HTPF test.*

$\sigma_{ij}$ corresponds to six unknowns, while one HTPF test yields only one data point, $\sigma_n(\underline{N})$, given that the components of the unit normal to the fracture plane are derived from geophysical logs.

In domains where linear spatial stress variation may be assumed (as in crystalline rocks), HTPF tests are conveniently integrated with true hydraulic fracturing tests for a complete stress determination.

But the linear approximation cannot be applied in most sedimentary formations in which the stress field varies non-linearly from bed to bed. In such formations, HTPF is found to be helpful for measuring the vertical stress component from tests on preexisting horizontal joints (see Section 3).

**• Hydraulic fracturing in inclined wells**

When the pressurized section of the well is inclined to all principal stress directions, the radial component ($\sigma_{\rho\rho}$) of the stress tensor at the borehole wall is a principal component ($\sigma_\rho$), which is equal to the applied pressure ($\sigma_\rho = P_w$). Here we reckon compression as being positive. The three other components are (e.g. Cornet [chapt.12], 2015) stated as:

$$\sigma_{\theta\theta} = \sigma_{11} + \sigma_{22} - 4[(\sigma_{11} - \sigma_{22})\cos 2\theta)/2 + \sigma_{12}\sin 2\theta] - P_w \qquad (2)$$

$$\sigma_{zz} = \sigma_{33} - 4\nu\,[(\sigma_{11} - \sigma_{22})\cos 2\theta)/2 + \sigma_{12}\sin 2\theta] \qquad (3)$$

$$\sigma_{\theta z} = 2\,(\sigma_{23}\cos\theta - \sigma_{31}\sin\theta) \qquad (4)$$

The two principal components that depend on the azimuthal coordinate θ, at the borehole wall, are respectively:

$$\sigma_M = 1/2\,(\sigma_{\theta\theta} + \sigma_{zz}) + [(\sigma_{\theta\theta} - \sigma_{zz})^2 + 4\,\sigma_{\theta z}{}^2]^{1/2} \qquad (5)$$

$$\sigma_m = 1/2\,(\sigma_{\theta\theta} + \sigma_{zz}) - [(\sigma_{\theta\theta} - \sigma_{zz})^2 + 4\,\sigma_{\theta z}{}^2]^{1/2} \qquad (6)$$

When pressure $P_w$ in the well is increased, the minimum principal stress $\sigma_m$ progressively declines until a hydraulic fracture is created normal to the local minimum principal stress component. This occurs for two symmetrical azimuths so that the fracture plane is inclined to the borehole axis. This often generates a set of parallel inclined hydraulic fractures called *en échelon* fractures (see Figure 4).

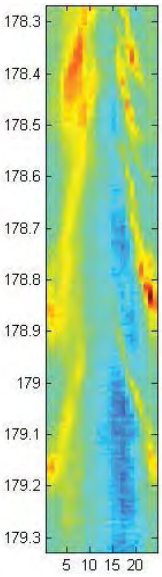

*Figure 4. Electrical image of en échelon fractures generated by hydraulic fracturing in a well inclined by more than 20° to any principal stress direction. The dip and azimuth of the fractures depend on all the far-field stress components. This is taken to advantage for evaluating the maximum horizontal principal stress magnitude when all other stress components are known (Cornet [chapt. 12], 2015)*

The azimuth Θ of the fractures depends on all the far field stress components and is such that the partial derivative of $\sigma_m$ with respect to Θ, $\sigma_{m,\Theta}$ , is null. When all the far field stress components but the maximum horizontal principal component, $\sigma_H$, are known, the measurement of the azimuth

of *en échelon* fractures yields a first equation for computing, $\sigma_H$ (Peska and Zoback, 1995). Another equation may be written by observing that these fractures do not support any shear stress. Hence, the geometry of *en échelon* fractures yields two equations for one unknown, and this ends up the complete stress determination.

### 2.3 Validation of the stress field characterization

- **Integration of results from geophysical logs and hydraulic tests**

Geophysical logs provide a tool for evaluating the validity of the continuity hypothesis inherent to a reliable regional stress field characterization. They help identify zones of main stress heterogeneity.

Each of the hydraulic tests provides results the uncertainty of which is assumed to be characterized by a normal distribution. Hence, they are described by an expected value and the associated standard deviation.

A measurement is considered to be homogenous with the proposed stress field characterization when its expected value rests within plus or minus two standard deviations from the predicted value (90% confidence level). When more than 30 % of the results are heterogeneous with respect to a proposed stress field characterization, validity of this characterization should be questioned.

- **Integration with focal mechanisms of induced seismicity**

Another means of ascertaining the validity of a stress field evaluation is provided by integration with data of different origins.

Such is the case when some local micro-seismic activity has been monitored so that some local focal mechanisms have been determined.

Micro-seismic sources are assumed to correspond to double couples characterized by their two nodal planes (see e.g. Cornet [chapt. 12], 2015). One of the nodal planes is the shear plane, and the normal to the other nodal plane yields the direction of slip in the shear plane. Assuming this unit vector is parallel to the shear stress component supported by the plane before seismic slip occurs, its orientation helps constraining four components of the local stress tensor: the three Euler angles that define the principal stress direction and a factor R that characterizes the ellipticity of the tensor:

$$R = (\sigma_2-\sigma_1)/ (\sigma_3-\sigma_1) \qquad (7)$$

where $\sigma_1$, $\sigma_2$, $\sigma_3$ are the principal stress components with $\sigma_3 \leq \sigma_2 \leq \sigma_1$ (Gephart and Forsyth, 1984; Maury et al., 2013).

When micro-seismicity results from large water injections in wells where hydraulic tests have been conducted, all results may be integrated for a common stress field evaluation.

This has been the case in the 1,000 m deep granite test site at Le Mayet de Montagne, France (Yin and Cornet, 1994). Some 22 HF and HTPF tests have been conducted in two vertical wells located some 100 m from one another. A total of 87 focal mechanisms have been determined within a volume equal to about $15x10^6$ $m^3$. A continuous stress field which varies linearly with depth has been found to be compatible with 95% of hydraulic tests but only 70% of the focal mechanisms.

It has been concluded that a regional stress field may be defined for this site. But 30% of the induced micro-seismic events occur in fractures that are inconsistent with this stress field. For those 70% that are consistent, identification of the slip plane provides means of determining the local pore pressure, since the local stress has been computed, with the assumption of an effective stress Coulomb slip criteria (Cornet and Yin, 1995).

## 3. A complete stress profile in the sedimentary Paris Basin (France)

ANDRA, the French agency in charge of developing a safe underground nuclear waste repository, is investigating the potential of the Callovo-Oxfordian argillite (mudstone) formation in the Paris Basin. This 200 m thick layer is interbedded between two carbonate units several hundred meters thick, namely the Dogger and the Oxfordian limestones.

An underground laboratory has been developed at a depth of about 500 m after an extensive regional stress field determination program had been conducted in various vertical and inclined boreholes near the small village of Bure. (see Figure 5. Wileveau et al. 2007; Cornet and Roeckel, 2012).

### 3.1 Borehole breakout analysis

Borehole breakouts have been observed in the Callovo-Oxfordian argillite in all boreholes drilled with water-based mud. But none were observed when oil -based mud was used for drilling. This clearly demonstrates the role of mud chemistry on the argilite mechanical behavior.

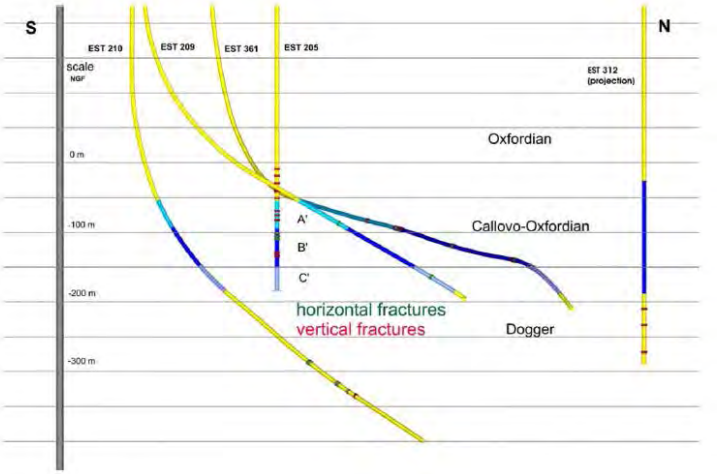


*Figure 5. Geometry of the various wells in which stress measurements have been conducted at Bure (depths are defined with respect to sea level) (Wileveau et al., 2007).*

### 3.2 Hydraulic tests in vertical wells

Various true hydraulic fractures have been conducted in vertical sections of the wells. They helped constrain the minimum horizontal principal stress (magnitude and direction).

For tests run with a stiff testing system, the breakdown pressure helped define an upper and a lower bound to the magnitude of the maximum horizontal principal stress depending on pore pressure effect.

Shut-in pressure values from a few HTPF tests run on horizontal joints provided the magnitude of the vertical stress component.

### 3.3 Hydraulic tests in inclined wells

Five of the six stress tensor components were known before running tests in the Dogger limestone. Hence, the geometry of *en échelon* fractures observed in the inclined section of the well helped determine the magnitude of the maximum horizontal principal stress in this formation.

Results of the complete stress determination are shown in Figure 6.

### 3.4 Pore pressure profile through direct in situ measurements

After the underground laboratory has been completed, detailed pore pressure measurements have been conducted in the argillite, as well as in the Dogger and the Oxfordian limestones (Figure 7; Delay et al., 2007).

Permeability for the argillite has been measured in the $10^{-19}$ – $10^{-20}$ $m^2$ range. Interestingly, the pore pressure in the Oxfordian limestone is hydrostatic but that in the Dogger limestone is lower than hydrostatic. This demonstrates that the Callovo-Oxfordian argillite layer is an efficient barrier to downward flow.

In addition, a parabolic profile has been identified in the argillite, but its origin is yet to be proposed. Indeed, as shown by Gonçalves et al. (2004), the osmotic hypothesis that has been proposed yields values that are much too low.

## 4. An orthotropic visco-poro-elastic model

### 4.1 Limits of elastic models

In the Paris Basin, orientations of borehole breakouts as well as that of true hydraulic fractures outline a remarkably uniform orientation for the maximum horizontal principal stress direction, i.e. N 155±10°E.

The present-day deformation rate is not given to direct observation, according to Nocquet (2012); velocities linked to present-day deformation are smaller than 1 mm/y. Further, no seismic activity is observed in the Paris Basin.

This has led Gunzburger and Magnenet to consider that the present-day stress field results from the long-term elastic response of the region following the last tectonic phase, namely the final "Alpine" activity occurring some 5 million years ago. Isotropic elastic moduli have been determined for the various layers so as to fit Wileveau et al.'s observed vertical stress profiles.

But Gonçalves et al. (2004) investigated the pore pressure variations generated by a poro-elastic response of the argillite layer to an Alpine push. They concluded that the overpressure in the argillite should have dissipated within the half million years following the end of the tectonic activity.

In addition, laboratory work on the mechanical behavior of the argillite (Zhang and Rothfuchs, 2004) has shown that the argillite exhibits a Burger type visco-elastic behavior (long-term fluid behavior). According to this observation, the shear stress component supported by the argillite, because of the "Alpine push", should have relaxed completely by now.

Hence, because of both the present-day shear stress and the pore pressure profile observed in the argillite, we conclude that a purely elastic model associated with an "Alpine push" leaves unanswered two key features of the argillite hydro-mechanical behavior.

Vertical seismic profiles that have been conducted in 2000 m deep wells, (some 100 km to the west of the Bure site), have outlined an orthotropic dynamic elastic behavior for both the Dogger and the Oxfordian limestones (Lefeuvre et al., 1992). Interestingly, detailed mapping of natural fractures in the various formations has outlined a significant density of vertical fractures oriented N155° E in both the Oxfordian and the Dogger limestones (André et al., 2006).

Hence, the dynamic elastic orthotropy of the materials is generated by the combination of sub-horizontal beds together with the vertical fractures field preferentially oriented N 155°E.

We observe that gravity alone acting on this orthotropic sedimentary formation may be the unique source of present-day stresses. But this leaves unanswered the two questions concerning the pore pressure and the shear stress in the fluid-type visco-elastic argillite.

### 4.2 A new orthotropic visco-poro-elastic model

In their attempt at modeling the vertical stress profiles observed in Bure, Günzburger and Cornet (2007), noticed that best fitting elastic parameters identified for the limestones were much lower than values computed from elastic waves propagation data derived from sonic logs. They concluded that a long-term softening process exists, affecting the limestone behavior, which is linked to pressure solution effects.

Natural fracture constitutes a preferred site for the development of pressure solution (Yasuhara and Elsworth, 2004; Renard et al. 2012). Micro-displacements are generated in the direction normal to the fracture planes. Hence, for a large fractured rock volume, pressure solution generates a rock volume decrease, the geometry of which depends on the fracture field morphology.

This observation has led Magnenet et al. (2017) to propose a simple hydromechanical model characterized by two main features linked to pressure solution effects. The first one concerns a time-dependent orthotropic mechanical behavior associated with pressure solution in fractures. The second one introduces a coupling term in the fluid mass balance equation involving volumetric strain because of the mass transfer from the solid to the fluid.

In closed systems, pressure solution stops when the ion concentration in the fluid near asperities gets smaller than a critical value that depends on local conditions (Yasuhara and Elsworth, 2004). Its time constant is considered to lie in the range $10^4$ to $10^5$ years.

The model has been implemented in a one D simulation with gravity loading only. (i.e., assuming no displacement in the horizontal direction and a Darcy law for the fluid flow.) Results are shown on Figures 6 and 7.

### 4.3 Influence of climate change on the present-day stress field

Because pressure solution stops after a certain time, it cannot explain by itself the present-day stress and pore pressure in the argillite.

Recent studies (Jost et al. 2007) have shown that cli-

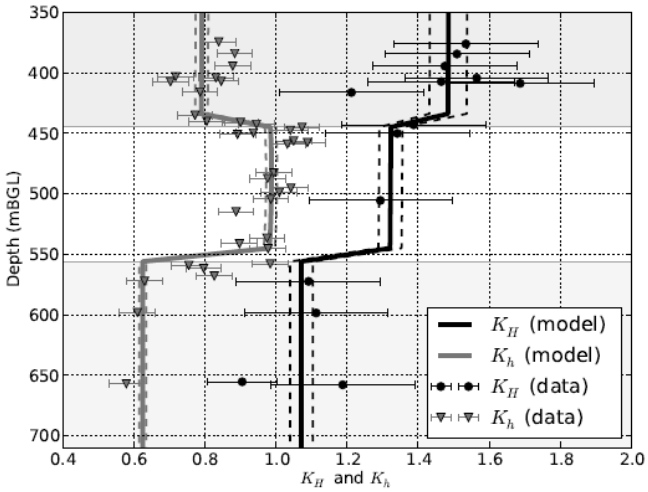


*Figure 6. Comparison between measured (dots with error bars) and computed values (continuous lines). Only the ratios $K_H = \sigma_H/\sigma_v$ and $K_h = \sigma_h/\sigma_v$ are plotted. The dotted lines on both sides of the continuous curves correspond to ± 10% variations of relevant elastic moduli.*

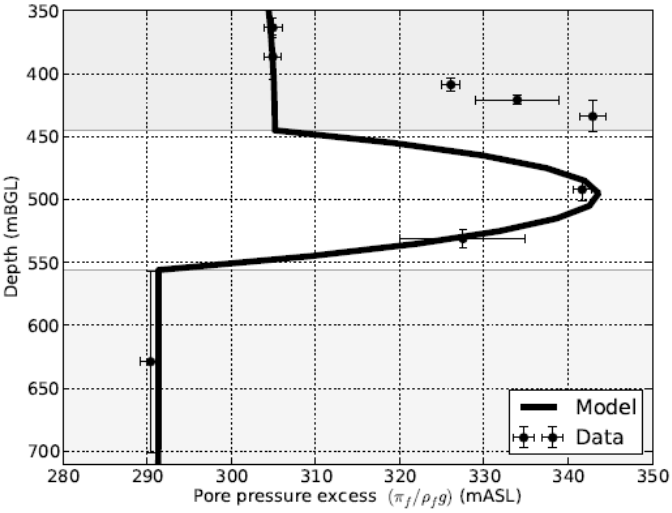


*Figure 7. Pore pressure profile near the underground laboratory.*

matic variations have influenced the local pore pressure down to the argillite in the Paris Basin. Indeed, because of permafrost development during the last glaciation, meteoritic water stopped percolating through the upper permeable layers. But the disappearance of permafrost some 13,000 years ago has let the meteoritic water percolation to resume. This resulted in some pressure gradients that induced deep fluid motion down to the argillite. This motion perturbed ions concentrations near asperities in fractures so that pressure solution has been reactivated within the last 10,000 years.

Such fluid motion variations occur with all glaciation cycles so that stresses in sedimentary formations may depend on climatic variations.

## 5. Conclusion: A new paradigm for intraplate stress fields

We may conclude that the present-day stresses and pore-pressure profiles in the argillite imply a present-day deformation, which is not linked to far field geodynamic conditions.

No seismic activity is observed in the Paris Basin. Some micro-seismicity is observed all around, yet the far field geodynamic conditions are the same for both locations. Interestingly, micro-seismicity is observed in old mountainous massifs, where meteoritic water may percolate quite deep, but it is absent in locations where impervious formations prevent this deep fluid circulation.

It is proposed that the regional stress field in the upper kilometers of intraplate regions is controlled by gravity alone, by the local materials rheology, and by fluid solid interactions associated with large-scale fluid circulations.

## References


André, G., B. Proudhon, H. Rebours, and Y. Willeveau. 2006. Paramètres contrôlant la distribution de la fracturation : exemple dans une série marno-calcaire du Jurassique. *C.R. Geoscience* ; 338, 931-941.

Berard, T., and F.H. Cornet. 2003. Evidence of thermally induced borehole elongation: a case study at Soultz, France*. Int. J. Rock Mech. Min. Sc*., 40, 1121-1140.

Cornet, F.H. 1993. The HTPF and the Integrated stress determination methods. In *Comprehensive Rock Engineering* (Hudson ed.); Vol 3, ch. 15, pp 413-432 Pergammon Press, Oxford

Cornet, F.H. 2015. *Elements of crustal Geomechanics*, 460 p., Cambridge University press.

Cornet, F.H., and B. Valette. 1984. In-situ Stress Determination from Hydraulic Injection Test Data; *J. Geoph. Res*.; 89( B13), 11,527 – 11,537.

Cornet, F.H., and J.M. Yin. 1995. Analysis of induced seismicity for stress field determination and pore pressure mapping*. Pure App. Geophys*., 145, 677-700.

Cornet F.H. and T. Roeckel. 2012. Vertical Stress profiles and the significance of stress decoupling; *Tectonophysics*; 581, 193-205.

Delay, J., M. Distinguin, and S. Dewonck. 2007. Characterization of a clay-rich rock through development and installation of specific hydrogeological and diffusion test equipment in deep boreholes. *Phys. Chem. Earth;* 32, 293-407.

Gephart, J.W., and D.W. Foryth. 1984. An improved method for determining the regional stress tensor using earthquale focal mechanisms data: application to the San Fernando earthquake sequence; *J. Geophys. Res.,* 89, 9305-9320

Gonçalves, J, S. Violette, and J. Wendling. 2004. Analytical and numerical solutions for alternative overpressuring processes: Application to the Callovo-Oxfordian sedimentary sequence in the Paris Basin, France. *J. Geophys. Res.,* 109, B02,110.

Gunzburger Y. and F.H. Cornet, 2007. Rheological characterization of a sedimentary formation from a stress profile inversion; *Geophys. J.int.*, **168**, 402-418.

Gunzburger, Y., and V. Magnenet. 2014. Stress inversion and basement-cover stress transmission across weel layers in the Paris Basin, France. *Tertonophysics*, 617, 44-57.

Haimson, B.C., and F.H. Cornet. 2003. ISRM suggested methods for rock stress estimation-Part 3: hydraulic fracturing (HF) and / or hydraulic testing of pre-existing fractures (HTPF*). Int. J. Rock Mech. Min. Sc*., 40, 1011-1050.

Ito, T., K. Evans, K. Kawai, and K. Hayashi. 1999. Hydraulic fracture reopening pressure and the estimation of the maximum horizontal principal stress*. Int. J. Rock Mech. Min. Sc*., 36, 811-826.

Lefeuvre, F., L. Nikoletis, V. Ansel, and C. Cliet. 1992. Detection and measure of birefringence from vertical seismic data: theory and application. *Geophysics,* 57, 1463-1481.

Lei, T., B.K. Sinha, and M. Sanders. 2012. Estimation of horizontal stress magnitudes and stress coefficients of velocities using borehole sonic data. *Geophysics*, 77, WA181-WA196.

Magnenet, V., F.H. Cornet, and C. Fond. 2017. A non-tectonic origin for the present-day stress filed in the Paris Basin. Submitted to *J. Geophys. Res.*

Maury, J., F.H. Cornet, and L. Dorbath. 2013. A review of methods for determining stress fields from focal mechanisms: application to the Sierentz 1980 seismic crisis (Upper Rhine Grabben); *Bull. Soc. Geol. Fr*., 184, 319-334.

Nocquet, J.M., 2012. Present-day kinematics of the Mediterranean: a comprehensive overview of GPS results. *Tectonophysics*, 579, 220-242.

Pesca, P., and M.D. Zoback. 1995. Compressive and tensile failure of inclined well bores and determination of *in situ* stress and rock strength*. J. Geophys. Res.,* 100; 12,791-12,811.

Renard F., K. Mair, and O. Gundersen. 2012. Surface roughness evolution on experimentally simulated faults. *J. Struct.Geol*., 45, 101-112

Wileveau, Y., F.H. Cornet, J. Desroche, and P. Blumling. 2007. Complete in situ stress determination in an argillite sedimentary formation *Phys. Chem. Earth*, 32, 866-878

Yasuhara, H., and D. Elsworth. 2004. Evolution of permeability in a natural fracture: significant role of pressure

Yin, J.M., and F.H. Cornet. 1994. Integrated stress determination by joint inversion of hydraulic tests and focal mechanisms*. Geophys. Res. Le*tt., 21, 2645-2648.

Zhang, C., and T. Rothfuchs. 2004. Experimental study of the hydromechanical behavior of the Callovo-Oxfordian argillite*. App. clay Sc.,* 26, 325-336.

Zoback, M.D. 2007. *Reservoir Geomechanicss*, 450 p., Cambridge University Press.

# Stress and Pressure in Mudrocks Bounding Salt Systems

*Submitted by Maria A Nikolinakou, The University of Texas at Austin, Austin, Texas*

## 1. Introduction

Understanding pore pressure and stress in geologic systems can provide valuable insights into the fundamentals of earth processes and is important for economic geology (hydrocarbon exploration, mining).

This article focuses on salt geologic systems. Salt is found in many parts of the world and is associated with significant energy resources. Salt systems can range from hundreds of meters to hundreds of kilometers. Because salt is a solid viscous rock, over geologic time it deforms into rising diapirs and spreading salt sheets. Geologic processes that contribute to the development of salt systems include deposition, porous-fluid flow, viscous salt flow and tectonic shortening or extension. Because these processes are time-dependent, the geomechanical characteristics of the bounding mudrocks also evolve with time.

Routinely, the study of geologic systems relies on kinematic restoration. This is an inverse method that recreates past geometries of a geologic system based on the present-day geometry. However, the poro-mechanical characteristics of sediments are not taken into consideration in the restoration process. Over the last two decades we have also seen significant advances in the mechanical study of static salt geologic systems. These studies introduced poro-mechanical principles, transient analyses, and three-dimensional geometries. Static analyses offer a very powerful tool for understanding the stress field around existing salt bodies, based on their present-day geometry. However, they cannot predict stress or pressure history, which is important for the present-day properties and stress state of the sediments.

We develop large-strain, transient, evolutionary geomechanical models that couple sedimentation with salt flow and porous-fluid flow (e.g., Figure 1). This coupling allows us to account for the effects of deposition, salt loading, and basin deformation on the development and dissipation of excess pore pressures. In addition, it enables us to understand the effect of excess pressures on the evolution of the geologic system.

## 2. Geomechanical models

We built transient evolutionary (forward) models using the finite element package Elfen®. The analyses are transient. The models are plane strain, and simulate the evolution of a salt wall (Figure 1). The salt and basin geometries are not kinematically prescribed. We simulate sedimentation by aggrading the top of the model to predefined deposition horizons (see Nikolinakou et al., ARMA 17-345; Heidari et al; ARMA 17-881). We model the salt as an impermeable solid viscoplastic material. Basin sediments are modeled as porous elastoplastic, using the SR3 critical-state constitutive model from the Elfen® material library. The consolidation properties are calibrated based on our high-stress experimental program on Gulf of Mexico mudrocks (research conducted at Tufts University).

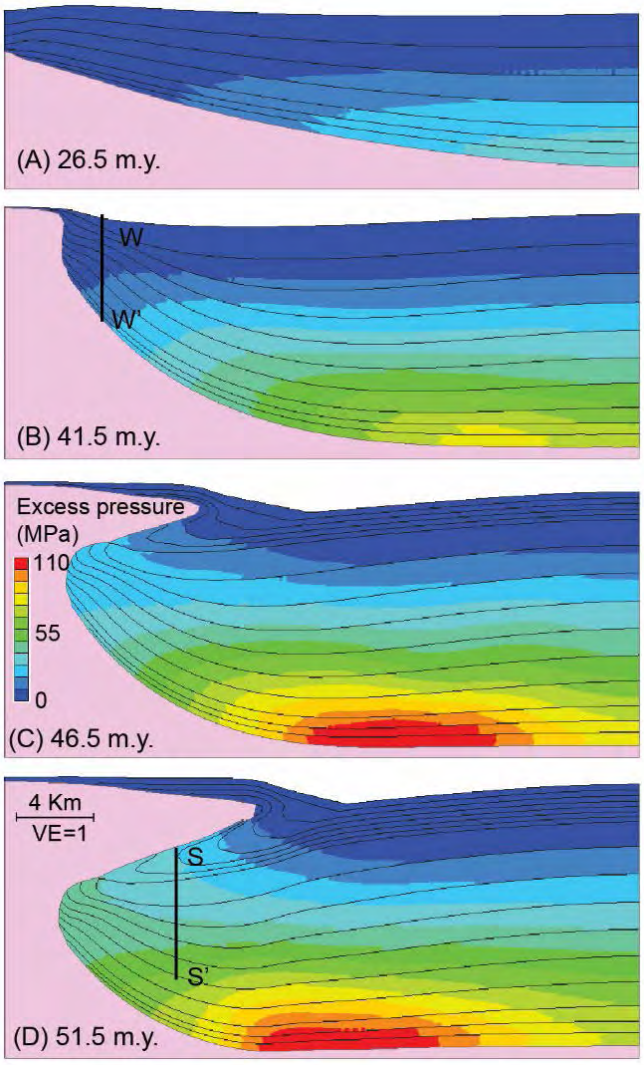


*Figure 1: Transient evolutionary model of a rising salt wall developing into a salt sheet. Contours show excess pressure that develops because of rapid sedimentation and loading from growing salt (Nikolinakou et al., ARMA 17-345).*

## 3. Key results

**3.1 Coupling salt movement and fluid flow.** When deformation is uniaxial (e.g., tectonically stable basins), sediment stress-strain behavior can be fully described as a function of vertical stress. Industry workflows, including pressure-prediction workflows, have been developed based on this uniaxial assumption. However, a deforming salt body may apply an additional, non-vertical load on depositing sediments. For example, a rising wall expands laterally and increases the horizontal stress in wall rocks (green solid vs. dashed line, Figure 2). When the coefficient of consolidation of the wall rocks is low, the salt rise results in excess pressures as the salt pushes laterally onto the sediments (solid blue line, Figure 2). These excess pressures are higher than those predicted by assuming a uniaxial sediment column with the same deposition rate as the wall rocks (dashed light blue line, Figure 2). The difference illustrates the contribution of salt loading.

The emplacement of the salt sheet (Figure 1) augments the development of excess pressures beneath salt in two ways: it imposes a growing external load (salt weight), and it increases the dissipation path. Because salt is impermeable, excess pore pressures need to dissipate to the front of the salt sheet; as the sheet length increases, so does the drainage path (Figure 1C, 1D).

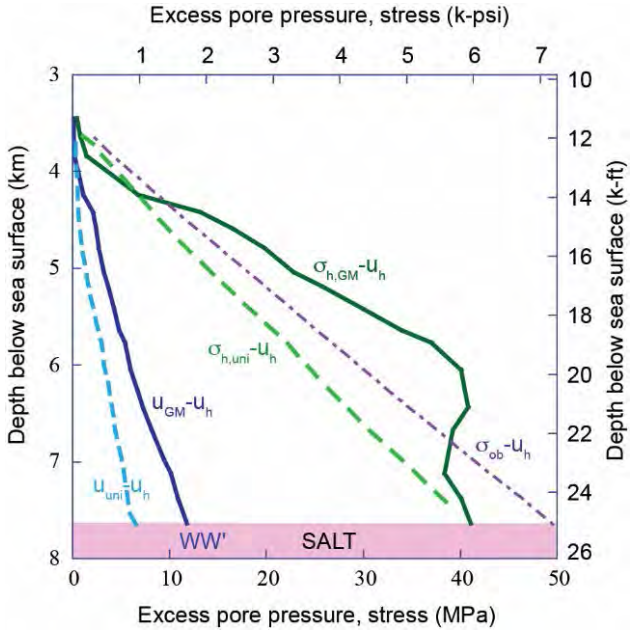


*Figure 2. Excess pore pressure and stress profiles along WW' (Figure1B). Excess pore pressure predicted by the geomechanical model ($u_{GM}$-$u_h$; solid blue line) is higher than that predicted by a uniaxial model for the same average sedimentation rate ($u_{uni}$-$u_h$; dashed blue line). This is because salt increases the horizontal stress in wall rocks (solid ($s_{h,GM}$) vs. dashed ($s_{h,uni}$) green lines). Reduced overburden ($s_{ob}$; dotted purple line) is shown for reference.*

**3.2 Coupling pore pressure and stress.** The high excess pressures developing below salt result in low effective stresses, despite the imposed salt weight. The direct consequence of low effective stresses is low sediment strength. We find that sediments are practically failing in a zone that extends several hundred meters below the base of salt (e.g., Nikolinakou et al., ARMA 17-345). Hence, our model results provide mechanisms that can explain the presence of shear or transition zones often reported below salt.

When drilling a borehole, mud is circulated to provide temporary support to the recently drilled, exposed section of the borehole before the cement job is completed. The mud weight needs to maintain pressure above the formation pore pressure to prevent flow into the borehole. However, this mudweight pressure should remain below the formation-fracture pressure to avoid fluid loss into the formation. The difference between the maximum mudweight that causes fracturing and the minimum one that controls the pore pressure is the drilling window. We find that the high excess pressures result in small drilling windows below salt. For example, in the model shown in Figure 1, the drilling window immediately after salt emplacement is less than 1 pound per gallon, for a considerable depth below the salt base (Figure 3).

Because we can predict the evolution of porosity with time, we can calculate an equivalent velocity field for any stage during the evolution of the system (e.g., Figure 4). We find that during salt emplacement, subsalt velocities do not reflect the weight of the overlying salt; in contrast, they remain low, comparable to velocity values near the mudline. This is because excess pressures support the salt weight, and there is little volumetric change (compression) within the mudrocks.

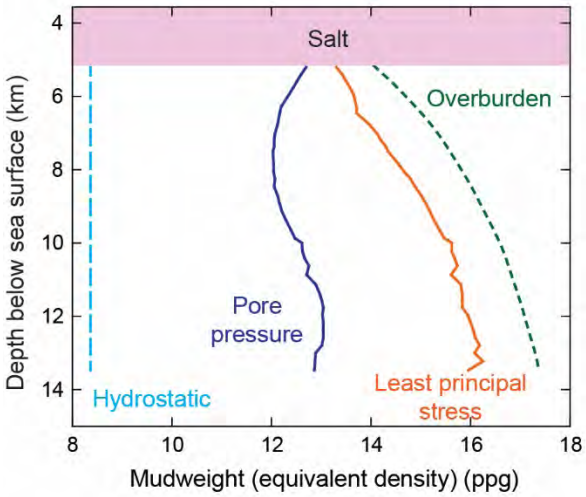


*Figure 3. Pore pressure and least principal stress gradients along vertical profile S-S below middle of salt sheet (shown in 1D).*

### 3.3 Effect of excess pressures on geologic evolution

We compare two salt systems (Figure 5): one with a sedimentary basin that is composed entirely of low permeability mudrocks (Figure 5A), and one with a basin that includes one highly permeable sand layer (Figure 5B). Except for the sand layer, the two models are identical. The permeable sand layer transmits excess pressures from deep sediments far from salt (D; Figure 5B) to shallow sediments near the salt wall (C; Figure 5B). The transmitted excess pressures result in low effective stresses near salt, and hence low strength. As a result, the roof of the system with the sand layer is weaker than the roof of the system with a uniform mudrock basin. After the same number of elapsed years, the salt system with the sand layer has developed further. In other words, by coupling salt flow with porous-fluid flow, we can predict a different geologic evolution.

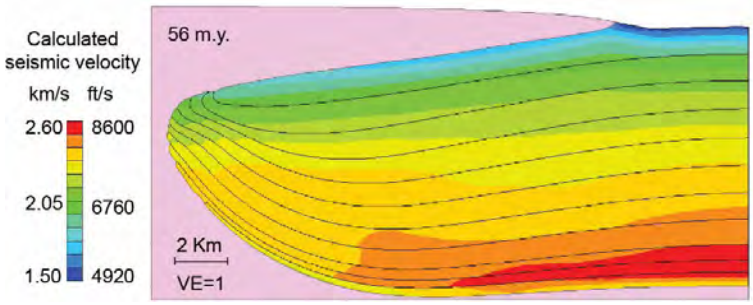


*Figure 4. Calculated velocity field below salt sheet with no roof.*

## 4. Further advances in pressure and stress prediction

Evolutionary models provide valuable insights into the change of stress and pressure with time; however, they are rarely able to simulate a specific field. In order to improve prediction around actual salt bodies, we have developed a workflow that couples geomechanical modeling with measured velocities (e.g., Heidari et al., Geophysics; Nikolinakou et al, ARMA 16-043). This workflow allows us to predict pressure and the full stress tensor based on present-day geometries, field measurements and geomechanical characteristics of a geologic system.

Geomechanical models (static or evolutionary) have advanced significantly. However the constitutive models describing sediments have been developed based on experiments made on near-surface materials. We are now studying geologic systems with scale and stress levels that are orders of magnitude different. Recent experimental work on Gulf of Mexico material has revealed a strong stress dependency in material behavior. We are now studying the form and evolution of the yield surface under high stress levels and complex geologic stress paths. Our challenge is to understand how compression, yielding and strength evolve along these complex stress paths, and to incorporate this more realistic behavior in pressure prediction workflows.

## 5. Key points

We develop transient evolutionary models that couple three geologic processes: salt deformation, basin sedimentation and porous fluid flow. These models allow us to study the kinematic evolution of a salt basin and predict how stress, strength, porosity and pore pressure evolve together with the geologic system. The models predict the full stress tensor and pore pressure with time and provide a predictive tool for drilling. Our results help advance our fundamental understanding of the interaction between pressure, stress, and deformation in basins. Furthermore, our modeling provides the foundation for a technical approach that can address many geological systems where large strains, pore fluids, and sedimentation interact.


## Acknowledgements

This study was funded by the Applied Geodynamics Laboratory (AGL) consortium, the UTGeoFluids consortium and the Jackson School of Geosciences, at the University of Texas at Austin.


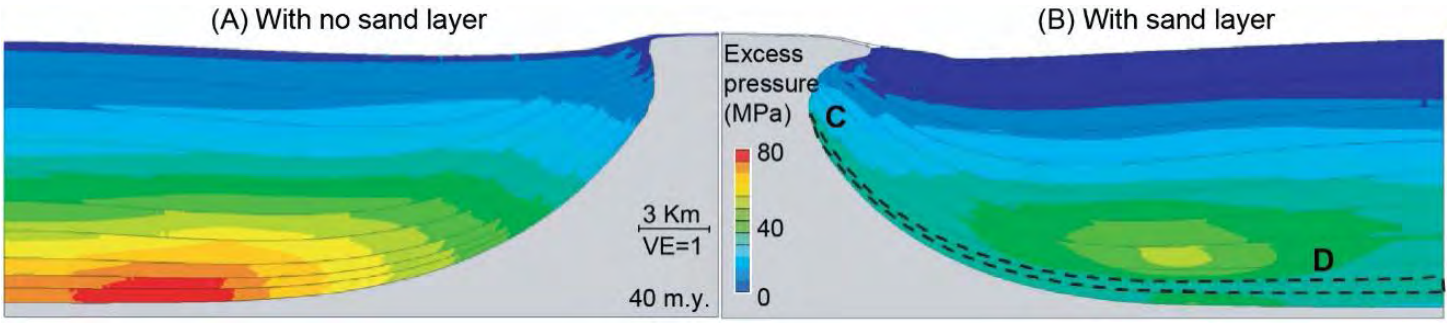


*Figure 5: System geometry and excess pressures in: (A) uniform salt basin consisting entirely of low permeability mudrocks; and (B) same basin as in A, but with a permeable sand layer (dashed line) (Heidari et al; ARMA 17-881).*

# Passive Seismic Tomography for Analysis of Stress Redistribution in Deep Mines

*Submitted by Erik Westman, PE, PhD, Professor and Department Head, Mining and Minerals Engineering, Virginia Tech, Blacksburg, VA,*

## 1. Introduction

Coal bumps and rock bursts have been a problematic issue for the underground mining community for many, many decades. The sudden release of highly-stressed rock from a mining face can result in injury or fatality of the underground workers. As mines continue to deepen, this induced seismicity is one of the most critical issues that must be addressed to ensure the safety and productivity of miners. Over the past four decades the use of seismic tomography has gradually developed to allow the identification and location of highly-stressed portions of a rock mass in the hopes that they could be de-stressed and safety thereby improved. This method provides additional information that can complement field observations, *in situ* measurements, numerical modeling, and other existing techniques. This summary describes a brief history of seismic tomography, the concept behind using p-wave arrival times for mapping stress redistribution, and two examples of its usage in deep mines.

In 1917 Johann Radon theorized that energy which was transmitted from one boundary of a body to another could be used to develop an image of the interior of the body. In the 1960's computational power became available so that this theory could be applied, and Computed Tomography (CT) became a new tool for the medical industry -- resulting in Nobel awards for Hounsfield and Cormack . Through the 1970's and 1980's the technology was gradually adapted to the geosciences, using seismic energy rather than the x-rays used by in the medical field.

## 2. Passive seismic tomography

This summary paper primarily discusses the application and results of travel-time tomography using the first arrival of the seismic wave (i.e. p-wave velocity tomography).

In seismic tomography the velocity with which seismic energy travels through a rockmass is analyzed. The seismic energy can either be from an active source (for example a hammer strike or a blasting cap) or from a passive source (either naturally-occurring or induced seismicity). Much excellent work was done related to underground hard rock mines by R. Paul Young and others in the use of seismic tomography using an active source. They showed that known stress redistribution in underground excavations could be imaged with p-wave velocity tomography.

Kissling et alia (1984) were some of the first to use passive seismic tomography for imaging the subsurface. They used the many naturally-occurring small crustal earthquakes to image the Long Valley Caldera in California, and referred to the approach as "Local Earthquake Tomography." The approach was subsequently used by others to image changes within the subsurface due to volcanism and petroleum reservoir imaging. The method was eventually adopted to mining, using mining-induced seismicity as the source for seismic energy. The highly-stressed volumes preceding a coal bump or rock burst became targets for using this gradually-maturing technology. In order to identify the highly-stressed portion of an underground mine there must be some relationship established between the induced stress in the rock and the velocity with which the seismic energy is transmitted through the rock. There is a generally monotonic relationship between induced stress and seismic wave velocity. The broad, general concept is that as the stress induced within the rock increases, microfractures are closed and the seismic wave travels at a higher velocity. This has been demonstrated in laboratory.

Tomographic inversion first discretizes the body of interest into volume elements ('voxels') and then adjusts the value assigned to the velocity of each voxel so that the root mean square difference between the measured and calculated travel times is minimized. The measured travel time is provided by the microseismic monitoring system typically in place at a deep mine, and the calculated travel time is determined by summing the times associated with an assumed raypath between the event and the sensor (i.e. the length of the raypath through a given voxel divided by the assumed velocity assigned to the voxel). The quality of the input data is paramount to obtaining reliable results; a typical plot of travel time versus distance between event and sensor is shown as Figure 1. This figure shows a typical background velocity of approximately 6 km/second with some

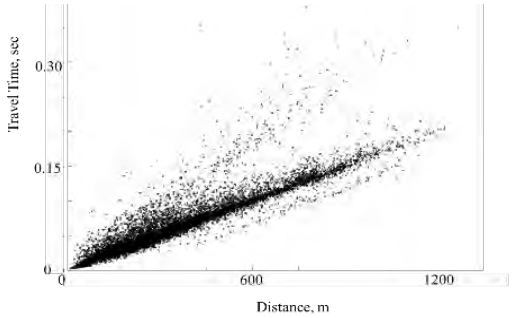


*Figure 1. Typical scatter plot of travel time versus distance between seismic event and geophone sensor; the inverse slope shows the velocity of the seismic ray with the majority of the rays traveling at approximately 6 km/sec.*

scatter due to variable geology, variable induced stress, and/or poor input data. Several methods are available for inverting the input data and solving for the velocity in each voxel, including least-squares regression, the simultaneous iterative reconstruction technique, conjugate gradient, and others.

## 3. Two examples

Several examples of using passive seismic tomography for time-lapse imaging of stress redistribution in deep mines have been published; two will be summarized here. The first example is from a deep longwall coal mine. The longwall coal mining method removes a one-meter thick slice of coal (typically 2-5 meters high) across a 300-400 m wide face. The overlying strata are allowed to cave behind the face and the miners and equipment at the face are protected by a series of hydraulic shields. Because the overburden is allowed to cave behind the face there is a highly-stressed forward abutment that exists within the coal just ahead of the mining face. This forward abutment makes an ideal target for validating the ability of passive seismic tomography to monitor stress redistribution, because the face location is well known in both time and extent. There has, however, remained a question about whether the caved strata behind the face are re-compacted under the loading of a "rear abutment."

Results from several days of a multi-week study at the longwall coal mine are shown as horizontal cross sections of the velocity distribution at the level of the mined seam in Figures 2-4. Figure 2 shows a high-velocity zone that corresponds to the location of the longwall face as it retreats through the deposit. This high-velocity zone is presumably due to the highly-stressed forward abutment. Figure 3 shows the velocity distribution along a line that is parallel to the mining face and 100 m into the caved zone. As expected, high velocity results correspond to the location of the pillars that remain on each side of the mined panel (and are thus highly-stressed) and a low velocity is displayed for the caved zone. When examining the results along a line that is perpendicular to the mining face (Figure 4) it can be seen that a high velocity zone 30 m ahead of the face indicates the location of the forward abutment; a low velocity zone from 40-200 m behind the face indicates the caved zone. Additionally, however, there is a relatively high velocity feature 200-250 m behind the face which indicates the likely rear abutment. This is significant because knowledge of the rear abutment's location and magnitude is beneficial for the mine engineers as they design pillars and ventilation, and for the rock mechanics community as they simulate loading at the mine level with numerical modeling. Further, the validation of the methodology provides confidence that it can be applied to monitoring the active face for anomalously-high stresses which may precede a coal bump.

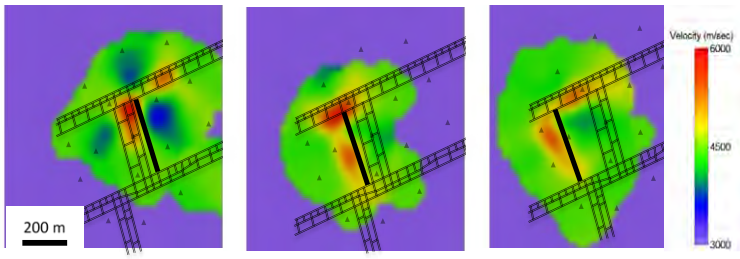


*Figure 2. Plan-view velocity tomograms at seam level. Pixels not traversed by rays are shown in purple. Face locations shown by solid black line. (Westman et al., 2012a)*

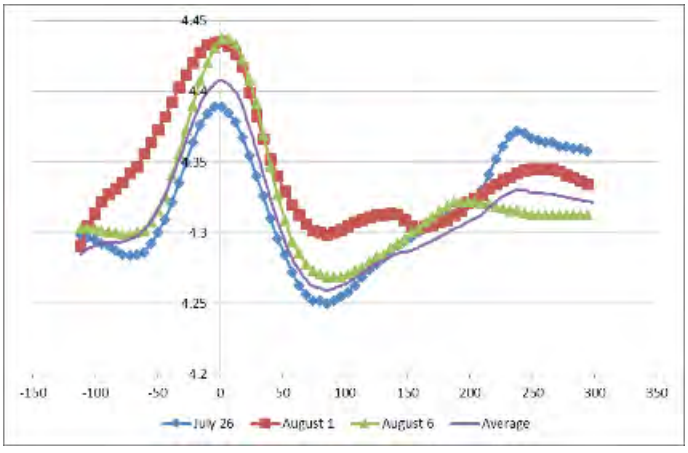


*Figure 3. Distribution of velocity parallel to the face and approximately 100 m into the face. The plots are all oriented such that the tailgate is positioned at a value along the x-axis of zero, so that the x values indicate a distance from the tailgate toward the headgate (meters). Values on y-axis are velocity, with units of km/sec. (Westman et al., 2012a)*

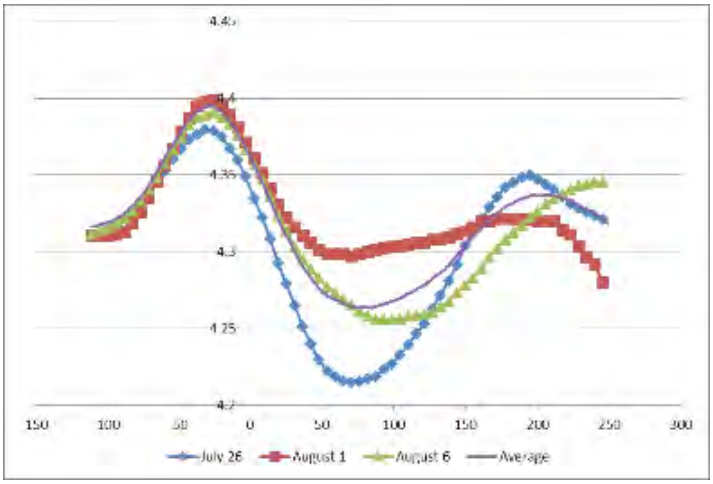


*Figure 4. Distribution of velocities parallel to gateroads, and at mid-face. The plots are all oriented such that the face is positioned at a value along the x-axis of zero, so that the x values indicate a distance into the face (meters). Values on y-axis are velocity, with units of km/sec. (Westman et al., 2012a)*

A second example of passive seismic tomography at a deep mine is from a block cave mine. Block cave mining occurs in a deposit that is very thick as opposed to the tabular coal seam discussed in the prior example. With this mining method, a two-dimensional horizontal slot is cut underneath the ore body, which must be relatively weak. The weak ore breaks as the slot is cut beneath it and then falls into collection points from which it is withdrawn. As more broken ore is withdrawn from the collection points the weak orebody continues to fracture and cave, falling into the collection points. In this example, a mine-wide microseismic monitoring system was already installed and was continuously monitoring the locations and magnitudes of the induced seismicity. This data set was then used as input for the passive seismic tomography.

Figure 5 shows results from a month when the undercut was being developed below the main orebody. In this figure the results are shown as a contour of relatively low velocity, indicating the location of the undercut and associated fractured or de-stressed rock. Approximately one year later, Figure 6 shows the development of the main block cave in the ore body. The large, low-velocity bulb is the fractured zone and a high-velocity zone overlies the cave, understood to be the seismogenic zone. A previously-mined portion of the ore body exists above the current block cave and a low-velocity result shows where it is now subsiding toward the current mining.

As with the longwall example, the results of the tomography provide mine engineers and geologists with valuable information. One of the biggest concerns with a block cave operation is the timing and extent of the block cave. Microseismic monitoring alone certainly helps to inform the size and shape of the cave but the passive seismic tomography provides a further tool for understanding stresses in the seismogenic zone and development of the cave. Additionally, the velocity distribution information can be used to help calibrate numerical models so that future performance at the mine can be modeled.

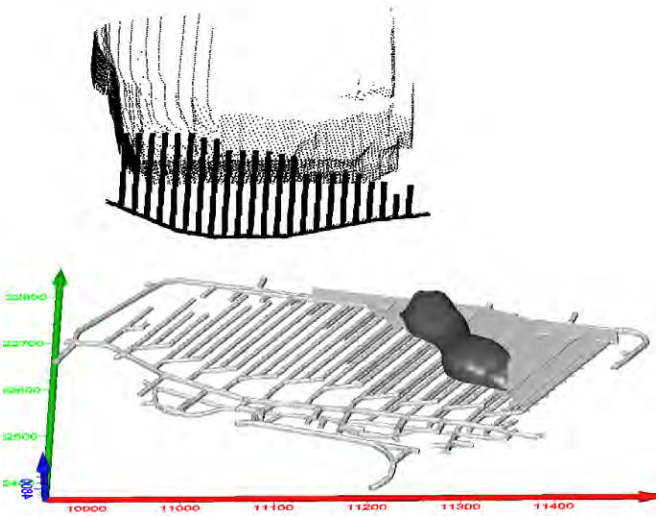


*Figure 5. Results from a month when the undercut was being developed below the main block cave orebody (a previously-mined zone is shown at the top of the figure). In this figure the results are shown as a contour of relatively low velocity, indicating the location of the undercut. Distance units, shown on axes, are in feet.*

## 4. Conclusions

Continued implementation of this method at deep mines has the potential to not only improve safety and efficiency at those sites, but also help the rock mechanics community better understand rock behavior on the mezzo- and crustal-scales. The advantages that mining operations have is that it is a mezzo-scale (not lab, not crustal), the location of the perturbation is well known, and the time scale is much shorter than that of crustal events. Thus, using the knowledge gained by this time-lapse, volumetric monitoring method can potentially help the rock mechanics community understand time-dependent rock mass behavior on the crustal scale as well.

Future developments with passive seismic tomography for stress redistribution monitoring include uncertainty quantification (using checkerboard method

and synthetic travel times), improved algorithms and solution times, and real-time implementation and notification at active mining operations. Each step provides valuable information that can further improve the safety and efficiency of mining operations.

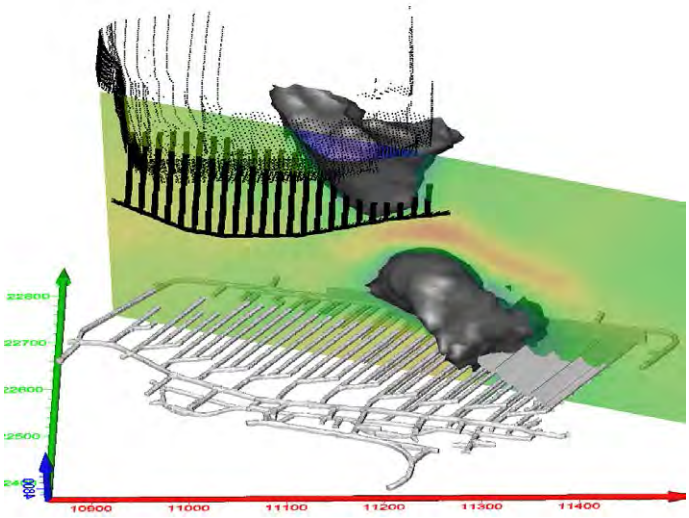


*Figure 6. The main block cave in the ore body. The low-velocity bulb is the fractured zone, and a high-velocity zone surrounds the cave, known as the seismogenic zone. A previously-mined portion of the ore body exists above the current block cave and a low-velocity result shows where it is now subsiding toward the current mining. Distance units, shown on axes, are in feet.*

# 2017 ARMA Workshop: Hydraulic Fracturing

*Submitted by Gang Han, Aramco Services Company; Chair, ARMA Technical Committee on Hydraulic Fracturing*

The 2017 ARMA Hydraulic Fracturing Workshop, organized by ARMA Technical Committee on Hydraulic Fracturing (TCHF), was held on June 25th in San Francisco, California, as part of activities preceding the 51st ARMA Rock Mechanics/Geomechanics Symposium. The goal was to clarify fundamental physics involved in hydraulic fracturing and demonstrate the validity of the models. Over 90 participants representing 70 organizations from 13 countries attended the workshop.

The workshop consisted of a morning session of lab and field findings and an afternoon session of model runoffs. The complete presentations are available to the Hydraulic Fracturing Community (HFC) members at the ARMA TCHF website (http://armarocks.org/sample-page/committees/technical-committee-on-hydraulic-fracturing-tchf-2/).

## Morning Session: Lab and Field Findings

Twelve invited speakers from four national laboratories, seven universities, and three industry affiliates participated in the Lab and Field Findings session. Investigations from various labs, field data from a deep mine, and from the Marcellus and Vaca Muerta fields revealed aspects of the fracturing physics.

Professor Bezalel Haimson(University of Wisconsin-Madison) opened the session with a comprehensive review of the hydraulic fracturing techniques applied to the measurement of in-situ stresses.

Dr. Curtis Oldenberg (Lawrence Berkeley National Laboratory) reported on employing this technique to characterize the ground stresses at the kISMET site, a 1450m deep mine in Lead, South Dakota. Ten organizations—from national labs, universities, and service providers—have used the kISMET test facility to advance stress field characterization, hydraulic fracture initiation and propagation, and induced seismicity monitoring, as well as pre-and post- fracturing simulations.

Based on the reviews of a series of lab experiments with natural and artificial rocks under realistic field conditions, Dr. Romain Prioul (Schlumberger) identified rock heterogeneity and lab-field scalability as accountable for the differences between experiments and models.

Dr. Jeff Burghardt (Pacific Northwest National Laboratory) proposed a methodology to address the lab scalability for a tight gas reservoir. A complex fracture pattern was observed in a true-triaxial test of a big block traversed by natural fractures.

*Fig. 1. The Organizing Committee and TCHF members (from left to right): Bill Carey, Sau-Wai Wang, Mukul Sharma, Thomas Doe, Gang Han, Ahmad Ghassemi, Joe Morris, Xiaowei Weng.*

Testing 13-inch granite cubes in a true triaxial apparatus, Dr. Ahmad Ghassemi (University of Oklahoma) revealed multiple mechanisms involved in hydraulic fracture propagation, including tensile, shear slip and dilation, mixed mode, etc.

Through imaging and acoustic emissions of fracturing with different preset flaw configurations, Dr. Bruno G. Silva (New Jersey Institute of Technology) identified both tensile and shear dominant fracture mechanisms, depending on the vertical loads.

Dr. Mukul Sharma (University of Texas at Austin) and his team demonstrated the importance of pore pressure on fracture propagation through controlled injection experiments.

Dr. Andrew Bunger (University of Pittsburgh) reported on achieving lower breakdown pressures due to "static fatigue", a phenomenon by which rock fails in a time-delayed manner at loads insufficient to induce instantaneous failure.

Several presentations focused on fracture permeabilities in natural and induced fractures. For Marcellus shales, Dr. Bill Carey (Los Alamos National Laboratory) found that in-situ stresses play a more important role in determining the permeability of natural fractures than subsequent reactivation or changes

in effective stress. For Vaca Muerta shales, Dr. Hamid Pourpark (Total) demonstrated significant variations of fracture permeabilities under different confining stresses, fluids, and proppants.

The investigations reported in this session advanced the understanding of the physics involved in hydraulic fracturing. The findings set the stage for the afternoon modeling session, in which the capability of models in capturing the physical mechanisms observed in the laboratory and field experiments was demonstrated.

## Afternoon Session: Model Runoffs

The afternoon session presented model runoffs that capture the physics of hydraulic fracturing. Some 20 fracturing models and seven benchmark case studies were presented. From simple to complex, the benchmark cases included:

1. Single fracture in homogeneous, elastic media.

2. Single fracture in layered, elastic formations.

3. Single fracture in homogeneous, poroelastic and thermoelastic media.

4. Single fracture in elasto-plastic media (low cohesion, low Young's Modulus).

5. Single fracture interacting with natural fractures and discontinuities (elastic, poroelastic).

6. Single fracture in layered elastic media with complex fluids (non-Newtonian, compressible).

7. Multiple competing fractures from perforation clusters (stress shadow effects).

The simplest Case 1 compared the numerical results with analytical solutions. Cases 2 to 5 highlighted the effect of rock complexity on fracture initiation and propagation. Case 6 evaluated the role of complex fluids such as $CO_2$ and foams. Case 7 studied the impact of stress interference between fractures.

The results obtained with the different models, as well as the comparisons among models, are documented in the workshop deliverables. In general, all the presentations demonstrated the ability of each specific model to capture various physics aspects of hydraulic fracturing. Differences among models arise from the different assumptions that each model uses, and also due to different, theoretical backgrounds, numerical approaches, incorporated physics, and other factors.

# 2017 ARMA Workshop: Emerging Advances in Geomechanics

*Submitted by Ghazal Izadi, Baker Hughes (a GE company)*

This workshop, organized by members of ARMA Future Leaders community, focused on multi-disciplinary problems of geomechanical engineering applications that require a deep understanding of complex physical phenomena, prediction of coupled hydro-thermo-mechanical processes, and handling of great amounts of scientific data. These applications include unconventional oil and gas production, mass mining processes, deep geothermal energy utilization, and underground storage of nuclear waste.

Presentations and discussions at the workshop were divided into four thematic sessions; 1) novel techniques in deep underground laboratories, 2) field characterization, 3) data analytics, and 4) novel numerical techniques.

This summary provides an overview of the presentations delivered at the workshop.

## Session 1: Novel techniques in deep underground laboratories

Dr. Yves Guglielmi (Lawrence Berkeley National Laboratory) offered his perspective on fault slip experiments in Underground Research Laboratories. His talk summarized results of field experiments at three different underground research laboratories to characterize fault zones hydromechanical properties as a function of their multi-scale architecture, and to monitor their dynamic behavior during the earthquake nucleation process. The outcome of these experiments provides a major contribution to a better understanding of aseismic and seismic slip, static and dynamic frictional fault properties and permeability increase.

Dr. Reza Jalali (Swiss Federal Institute of Technology (ETH)) discussed the in-situ Stimulation and Circulation Experiment at the Grimsel Test Site. This talk provided insights from a recently conducted decameter-scale hydraulic stimulation experiment, conducted at the test site in Switzerland. The experiment was designed to address important questions associated with the hydro-seismo-mechanical behavior of enhanced geothermal systems. The most relevant processes (e.g. shear dilatancy, seismic and a seismic slip front propagation, fracture conductivity changes, etc.) during fluid injection could be measured at a high spatial and temporal resolution.

## Session 2: Field characterization

Dr. Andrew Hyett (Yieldpoint Inc.) addressed the topic of time dependent rock mass behavior in deep hard rock mines. In this talk, a new framework for the interpretation of time-dependent deformation measurements in deep hard rock mines was introduced, followed by the application of "time series analytics" to extensometer data. His discussion also focused on whether such data sets can be used to "train" numerical models, potentially in real time, in order to enable those models to forecast excavation performance.

Dr. Robert Hurt (Pioneer Natural Resources) talked about developing inputs for advanced hydraulic fracture models. He emphasized that development of robust and quantitative model inputs is required to enhance a 3D hydraulic fracture model's utility. Some of the challenges in developing modeling inputs in the context of field scale applications were reviewed, followed by examples of how reduced order models, scaling, and effective parameters can be leveraged to derive 3D numerical model inputs.

Dr. Debbie Senesky (Stanford University) discussed "Gallium Nitride: A Platform for Extreme Environment Sensors and Electronics." Gallium nitride (GaN) has been utilized to facilitate the use of sensors and electronics in extreme environmental conditions such as those encountered in the oil and gas, geothermal, and space exploration industries.

## Session 3: Data analytics

Dr. Mario Costa Sousa (University of Calgary, Canada) offered his perspective on "Fast & Scalable Context-Aware Prototyping of Static and Dynamic Models of Subsurface Environments – A Change of Paradigm."

Dr. Stephan Arndt (Monash University, Australia) offered his perspective on "Bridging the Gap Between 3D Geomechanics, Modelling and Machine Learning." He reported the progress made in 3D geomechanics resulting from an increase of amounts of computed data. Such data, generated in finely gridded 3D models often containing tens of millions of points, allows the process of results interpretation by the user with only significantly limited possibilities. Fully coupled models linking draw schedule, flow modeling and geomechanics can be used for optimization and risk

analysis once workflows are fully automated.

Dr. Mehdi Maasoumy (C3 IoT) discussed the utilization of advanced analytics and machine learning to optimize productivity in oil & gas operations. His talk provided insight on the integration of disparate data sources – such as daily sensor readings from in-field equipment, unstructured data (e.g., field notes, operator comments, and maintenance logs from maintenance work orders), production logs, well attributes, and seismic survey data – to create a unified federated data image. This comprehensive data integration and platform gives data scientists the capability to rapidly iterate and refine machine learning models and deploy them to production in real time. In addition, the discussion focused on identifying the key design and operating parameters affecting the performance and failure of individual wells, in order to understand and then extend their lifetime going forward.

## Session 4: Novel numerical techniques

Dr. Bryan Tatone (Geomechanica Inc., Canada) presented an innovative, computationally-efficient simulation tool for rock fracturing applications in geomechanics. The finite-discrete element method (FDEM) explicitly simulates brittle fracture and fragmentation processes in discontinuous rocks. To overcome computational limitations, the new approach takes advantage of the computational power of modern graphics processing units (GPUs) using innovative high performance computing (HPC) and parallelization techniques. Application examples from the civil engineering, oil & gas, and mining industries include the assessment of excavation damaged zone around underground excavations, simulation of the geomechanical response of discontinuous reservoirs subjected to fluid injection, and analysis of structurally-controlled rock mass failure in large open pit mines.

Dr. Randolph R Settgast (Lawrence Livermore National Laboratory) talked about finite element/finite volume modeling hydraulically driven fractures in 3-dimensions. To illustrate the flexibility and effectiveness of the proposed approach when applied to real-world problems, several field scale case studies were presented.

Dr. Adriana Paluszny (Imperial College, UK) suggested Isogeometry as a step change for computational rock mechanics. Isogeometry is a novel numerical method that directly solves partial differential equations on the differential geometry of a body. It proposes a new manner of discretization (and reduces computational time), while increasing accuracy by combining geometry, discretization, and interpolation into one object, a Non-Uniform Rational B-Spline (NURBS). Its advantages can potentially be applied in the field of rock mechanics.

# 2017 ARMA Workshop: How Laboratory Geo-mechanics Testing Adds Value to Exploration and Production

*Submitted by Abhijit Mitra, Geomechanics Consultant, Metarock Laboratories, Houston, Texas.*

This half-day workshop was well-attended with an audience consisting of academicians and industry professionals from various countries. The single presenter at the workshop was Abhijit Mitra, a professional with more than ten years of experience in laboratory geomechanics. The workshop began by introducing the topic of geomechanics and how it impacts operations involved in hydrocarbon recovery.

Starting from prevention of well blowout to designing an effective reservoir stimulation strategy, principles of geomechanics have been used frequently in exploration and production of hydrocarbons in the past few decades. In recent years, depletion of existing plays demands that hydrocarbon producers be prepared with proper technology and innovations suitable for enhanced recovery. These require a solid understanding of fundamental principles, methodology and application of geomechanics on the part of reservoir engineers involved in exploration and production.

The collection of right input parameters is critical to success of any geomechanics study. The usual practice involves extracting information from measurements conducted via wireline sonic tools and/or seismic studies. However, these geophysical measurements need be validated against direct laboratory-measured values. Key components of a geomechanics study were presented along with the various data sources used in such study. Following this, the topic of laboratory geomechanics was introduced, presenting the steps to be taken before proceeding into a study as well as a detailed description of equipment being used. A number of standard and specialized geomechanics testing techniques were presented followed by instructions on how to conduct quality control of test results. The subsequent section focused on how to design a laboratory geomechanics program for a specific reservoir or operating environment. Finally, a few examples of laboratory geomechanics studies benefitting exploration and production activities were provided.